Remote Sens. **2014**, *6*, 2176-2194; doi:10.3390/rs6032176

OPEN ACCESS

remote sensing

ISSN 2072-4292

www.mdpi.com/journal/remotesensing

Article

Evaluating the Potentials of Sentinel-2 for Archaeological Perspective

Athos Agapiou [1,*], Dimitrios D. Alexakis [1], Apostolos Sarris [2] and Diofantos G. Hadjimitsis [1]

[1] Laboratory of Remote Sensing and Geoinformatics, Department of Civil Engineering and Geomatics, Cyprus University of Technology, Saripolou 2-8, Limassol 3603, Cyprus; E-Mails: dimitrios.alexakis@cut.ac.cy (D.D.A); d.hadjimitsis@cut.ac.cy (D.G.H.)

[2] Laboratory of Geophysical-Satellite Remote Sensing & Archaeoenvironment, Institute for Mediterranean Studies, Foundation for Research & Technology-Hellas (F.O.R.T.H.), Nik. Foka 130, Rethymno, Crete 74100, Greece; E-mails: asaris@ret.forthnet.gr

***** Author to whom correspondence should be addressed; E-mail: athos.agapiou@cut.ac.cy; Tel.: +357-25-002-471; Fax: +357-25-002-769.

Received: 15 January 2014; in revised form: 14 February 2014 / Accepted: 24 February 2014 / Published: 10 March 2014

Abstract: The potentials of the forthcoming new European Space Agency's (ESA) satellite sensor, Sentinel-2, for archaeological studies was examined in this paper. For this reason, an extensive spectral library of crop marks, acquired through numerous spectroradiometric campaigns, which are related with buried archaeological remains, has been resampled to the spectral characteristics of Sentinel-2. In addition, other existing satellite sensors have been also evaluated (Landsat 5 Thematic Mapper (TM); Advanced Spaceborne Thermal Emission and Reflection Radiometer (ASTER); IKONOS; Landsat 4 TM; Landsat 7 Enhance Thematic Mapper Plus (ETM+); QuickBird; Satellite Pour l'Observation de la Terre (SPOT); and WorldView-2). The simulated data have been compared with the optimum spectral regions for the detection of crop marks (700 nm and 800 nm). In addition, several existing vegetation indices have been also assessed for all sensors. As it was found, the spectral characteristics of Sentinel-2 are able to better distinguish crop marks compared to other existing satellite sensors. Indeed, as it was found, using a simulated Sentinel-2 image, not only known buried archaeological sites were able to be detected, but also other still unknown sites were able to be revealed.

Keywords: Sentinel-2; crop marks; Archaeological Index; archaeology; remote sensing archaeology

1. Introduction

1.1. Remote Sensing for Archaeological Perspective

The use of remote sensing techniques has revealed several possibilities from an archaeological perspective. A number of different satellite or aerial sensors have been already employed in a variety of archaeological applications, ranging from the identification of spectral signatures within archaeological sites, as well the mapping of the probability (risk) of archaeological sites. The results of these applications have been employed to manage and to protect the archaeological sites [1–5].

Moreover, remote sensing has been proven to be very useful in preparing an intensive survey campaign or directing fieldwork. Viewing archaeological structures from a ground level generally does not clearly identify the spatial characteristics of these structures, or the relationship to surrounding archaeological sites. In some cases, ancient structures are not apparent from ground level but become obvious from Earth observation techniques [6]. In addition, proper understanding of the recent and historic changes of the archaeological record might assist to construct contingency plans and management strategies to protect the archaeological heritage of a vulnerable area [7].

Several important archaeological discoveries have been made through the integration of remote sensing to current archaeological perspective and practice. Remote sensing, as well as other non-destructive methods have been widely used for discovering and mapping visible and buried archaeological remains [8–14]. Near-surface archaeological remains can be discovered due to detectable changes in vegetation growth, termed crop marks [15–19].

Such archaeological crop marks may be observed by exploiting vegetation indices, which are widely used in order to monitor the seasonal or even long-term variations of structural, phenological, and biophysical parameters of land surface vegetation cover [11]. Recent studies argue that there are many complex factors involved in the capturing of crop marks. For instance, the characteristics of the buried features, as well the soil characteristics, or even climatic and environmental parameters, can affect the formation of crop marks. Furthermore, the formation of crop marks is a dynamic phenomenon which may vary in each crop's phenological cycle [20–25]. Therefore, a better understanding regarding the formation of crop marks is needed based on remote sensing data.

Monitoring fluctuations of the Red and near infrared (NIR) spectrum during crop's phenological cycle is a key parameter to the detection of archaeological remains using remote sensing techniques. Current studies have shown that the spectral characteristics of satellite sensors—further to their spatial resolution—are very important for the detection of archaeological crop marks. According to [21], Relative Spectral Response (RSR) filters of sensors are one of most significant parameter for the detection of crop marks using satellite images In addition, multi-temporal satellite images can be also used for the detection of crops phenological changes due to the existent of buried archaeological relics [26,27], while airborne hyperspectral data can be also applied for supporting archaeological perspectives [4,28].

The selection of specific spectral bands for the detection of archaeological remains both in vegetated, as well under bare soil has been recently discussed by [29]. Indeed, as was found by [30], in cases where the dominant land cover over archaeological sites is known, then the optimal spectral range can be selected in order to improve the efficiency of archaeological observations using remote sensing data. Finally, the hyperspectral Archaeological Index has shown that the use of the spectral region around 700 nm and 800 nm can be effectively used for the enhancement of crop marks in vegetated areas [20,31].

1.2. Objectives

Spectral and temporal characteristics of the forthcoming Sentinel-2 dataset can provide new potentials for the archaeological perspective. The five-day temporal window of the Sentinel-2 sensor will give scientists the opportunity for a more detailed and systematic observation of vegetation marks, while its spectral bandwidth (Band 5 and Band 7) is very closed to the optimum spectral regions (700 nm and 800 nm) for the exposure of crop marks. Indeed, Sentinel-2 datasets are expected to be very useful for archaeological applications since their free distribution, along with their contribution to the continuity and improvement of Landsat series, will provide scientists with new acquisitions of images of archaeological sites all over the world.

This study aims to highlight the technological advantages of the Sentinel-2 sensor, as well as to inform the remote sensing archaeological community for the arrival of Sentinel-2 data in the near future. Moreover, the study aims to explore the capabilities of remote sensing sensors for the detection of new archaeological sites using simulated Sentinel-2 data. In addition, an evaluation of the capabilities of Sentinel-2 with other existing satellite datasets, widely used in archaeological perspective, has been also examined. For the aims of this study several existing vegetation indices have been evaluated, as well several other existing satellite sensors have been compared with the forthcoming Sentinel-2.

2. Methodology

The Sentinel-2 aims to provide continuity to services relying on multi-spectral, high-spatial-resolution optical observations over global terrestrial surfaces. It should be noted that the design of the Sentinel-2 mission aims at an operational multi-spectral Earth-observation system that complements the Landsat and SPOT observations and improves data availability for users [32]. In addition to high operational ability, the acquired data and potential products of the Sentinel missions also offer significant scientific opportunities, such as global coverage, long-term continuity, careful calibration of the satellite sensors, and a broad variety of remote sensing methods [33]. The spatial and temporal characteristics of the new Sentinel missions, primarily designed to provide routine multidisciplinary observations for operational services, are also very suitable for addressing some of the challenges associated with advancing Earth System sciences. The Sentinels are ensuring long-term observational commitment and will operate a range of instruments with different spectral bands and spatial resolutions with global coverage and high revisit times [34].

Furthermore, frequent revisits of five days at the equator require two identical, Sentinel-2 satellites operating simultaneously favoring a small, cost effective, and low-risk satellite. The orbit is

Sun-synchronous at 786 km altitude with a 10:30 a.m. descending node. This local time was selected as the best compromise between minimizing cloud cover and ensuring suitable sun illumination. It is close to the Landsat local overpass time and matches SPOT's, allowing the combination of Sentinel-2 data with historical images to build long-term time series. The 13 spectral bands span from the visible (VIS) and the NIR, to the short wave infrared (SWIR), at different spatial resolutions at the ground ranging from 10 to 60 m [33]. Spectral characteristics of Sentinel-2 are shown in Table 1.

Table 1. Spectral characteristics of Sentinel-2 sensor [35].

Band		Center	Spectral Width	Min 5%	Max 5%
		λcenter nm	Δλ nm	$\lambda_{min5\%}$ (± nm)	$\lambda_{min5\%}$ (± nm)
B	1	443	20	418.7	467.3
B	2	490	65	430.1	549.9
B	3	560	35	515.2	604.8
B	4	665	30	622.8	702.2
B	5	705	15	680.0	717.0
B	6	740	15	725.0	758.0
B	7	783	20	745.7	807.3
B	8	842	115	764.5	919.5
B	8a	865	20	835.0	895.0
B	9	945	20	907.7	977.3
B	10	1375	30	1342.6	1407.5
B	11	1610	90	1546.0	1685.0
B	12	2190	180	2045.0	2301.0

For the aims of this study, several ground spectroradiometric measurements taken over a control archaeological environment have been used. Firstly, the spectral signatures of barely crops taken during a complete phenological cycle have been spectrally convolved to the Sentinel-2 sensor using the appropriate RSR filters. Then, the data have been compared with other existing medium and high resolution satellite sensors. In detail medium resolution satellite images such as the Landsat series dataset (4 TM; 5 TM; and 7 ETM+), SPOT 5, as well as the ASTER sensor have been explored. Furthermore high-resolution satellite sensors have been also examined, including IKONOS, QuickBird, GeoEye, and WorldView-2. For all those sensors, their appropriate RSR filters have been used as shown in Equation 1. The RSR filters for each sensor were obtained from different sources: published data, (WorldView-2); the operator's websites (GeoEye-1, IKONOS, Landsat 7 ETM+, Landsat 5 TM, Landsat 4 TM, ASTER); and personal communication (QuickBird). The RSR filters of Sentinel-2 were provided by European Space Agency (ESA).

$$Rbandi = \Sigma (Ri * RSRi) / \Sigma RSRi \quad (1)$$

where:

Rbandi = reflectance at a range of wavelength (e.g., NIR Band).

Ri = reflectance at a specific wavelength (e.g., R 700 nm).

RSRi = Relative Response value at the specific wavelength.

The Sentinel-2 simulated dataset as well the other simulated datasets from the rest of the sensors have been compared with the hyperspectral Archaeological Index (see [20,31]) in terms of their performance from the archaeological perspective. The latest index has already been found to be very promising and suitable for the detection of vegetation marks using hyperspectral satellite data. Moreover, thirteen vegetation indices have also been evaluated for their performance. Finally, a simulated Sentinel-2 image, based on EO (Earth Observation)-Hyperion dataset (merged with high-resolution IKONOS image), has been studied in terms of photointerpretation and detection of crop marks.

3. Resources and Study Areas

The need for systematic monitoring of crop marks spectral signatures, related with subsurface remains, led to the creation of an archaeological test field in Cyprus [20]. The extensive test field is located in the central region of Cyprus, near the Alampra village (WGS 84, 36 ℕ: 535051, 3870818, Figure 1). For this purpose, local stone was placed in different depths and then covered with soil. Then, the topsoil was cultivated with dense vegetation (barley and wheat) in order to study the variations of the spectral signature of the crops as a result of the existence of subsurface remains. The main purpose of this field is to explore further characteristics of the crops spectral signatures' profiles throughout the phenological cycle of vegetation.

Figure 1. Photo taken from the archaeological test field in Alampra, Cyprus (WGS 84, 36 ℕ: 535051, 3870818). Formation of crop marks is shown in the photo with an arrow.

Several ground spectroradiometric measurements were taken during the whole crops phenological cycle using the GER 1500 handheld spectroradiometer. Over twenty *in situ* campaigns were performed during the sowing period until harvesting (complete phenological cycle). GER 1500 instrument has the capability to record spectral signatures in the visible (Vis) and very near infrared (VNIR) part of the spectrum (450–900 nm). Moreover, the specific spectroradiometer can record electromagnetic radiation within a bandwidth sampling of ≈1.5 nm. In total, more than 1700 ground measurements were collected over vegetation marks and the surrounding vegetated area ("healthy" area). A reference

spectralon panel was also used in each campaign to measure the incoming solar radiation and therefore calibrate the *in situ* measurements during the campaigns [36,37]. These spectral signatures were used in order to evaluate the potentials of the Sentinel-2, as well to compare the forthcoming sensor to other, existing available satellite images.

In addition a simulation of the Sentinel-2 product was attempted. For this reason, an EO-Hyperion image was used over the *Thessalian* area in Northern Greece. The *Thessalian* region is considered as the primary agricultural area of Greece. At this plain many of Neolithic settlements/tells called magoules were established from the Early Neolithic period until the Bronze Age (6000–3000 BC). The magoules are typically low hills of 1 to 5 m height and they mainly consist of loam and mud-based materials. Hundreds of magoules are located all over *Thessaly* and can be found within different kinds of vegetation. Due to the intensive cultivation of the land in the past and their low elevation, a major number of them are not clearly visible from the ground [3,38].

4. Results

4.1. Spectral Characteristics of Sentinel-2 from Archaeological Perspective

All ground narrowband reflectance values were resampled according to the Sentinel-2 spectral characteristics as well with the rest of the sensors examined in this study. Figure 2 shows the spectral bandwidth of the sensors, mentioned in this study, compared to a typical spectral signature of crop mark and healthy crop. In detail, this figure shows the spectral bandwidth of the Red—NIR part of the spectrum for Sentinel-2 (Bands 4–8); Sentinel-2 (Bands 5–7); Landsat 5 TM (Bands 3–4); ASTER (Bands 2–3); IKONOS (Bands 3–4); Landsat 4 TM (Bands 3–4); Landsat 7 ETM+ (Bands 3–4); QuickBird (Bands 3–4); SPOT (Bands 2–3); and WorldView-2 (Bands 5–7).

It is interesting to note that the spectral bandwidth of all the sensors is quite different. Not only is the spectral bandwidth is dissimilar, but, also, the central wavelength (indicated with blue line in Figure 2) is not the same. Therefore, as is indicated, all sensors might have similar, but not identical, spectral resolutions. This observation has prompted to investigate, if the capability of the Sentinel-2 sensor to "capture" information regarding vegetation marks can provide scientists with better results compared to other existing satellite data. The Sentinel-2 sensor has been designed to record vegetation characteristics using five different spectral bands (Band 4–8a). Indeed, some promising results indicating significant relationships of vegetation characteristics with the Sentinel-2 sensor have been already discussed [39,40].

As it was found from previous studies [21], IKONOS spectral sensitivity was able to enhance better vegetation marks compared to other medium- and high-resolution satellite sensors. Indeed, IKONOS RSR filters better distinguished buried archaeological remains as a result of differences in healthy and stress vegetation (approximately 1–8% difference in reflectance of the Red and NIR band and nearly 0.07 to the Normalised Difference Vegetation Index (NDVI) profile). This difference exceeds the relative uncertainties of calibration that ranges within 5% for satellite sensors according to relevant literature [41]. Moreover, the ASTER sensor was able to provide similar outcomes.

IKONOS and ASTER better performance for the detection of buried relics—compared to the rest of the sensors—was due to their spectral similarity with the optimum spectral regions for monitoring crop

marks. As is clearly shown in Figure 2, both IKONOS and ASTER central wavelengths of Red and NIR bands are very close to 700 nm and 800 nm, which are considered as the optimum spectral wavelengths for the detection of crop marks [20,31,42]. However, Sentinel-2 RSR filters appear more capable for the detection of buried archaeological features.

Figure 3 shows the RSR filters of the Sentinel-2 (Bands 1–8a) along with two typical spectral signatures of vegetation marks and healthy crops. Central bandwidth of Bands 5 (705 nm) and 7 (783 nm) are very close to 700 nm and 800 nm (optimum spectral regions for archaeological perspective) and, consequently, can be used in order to detect vegetation marks using remote sensing data.

Figure 2. Spectral bandwidths of the Red–NIR for different sensors used in this study: Landsat 5 TM (Bands 3–4); Sentinel-2 (Bands 4–8); Sentinel-2 (Bands 5–7); ASTER (Bands 2–3); IKONOS (Bands 3–4); Landsat 4 TM (Bands 3–4); Landsat 7 ETM+ (Bands 3–4); QuickBird (Bands 3-4); SPOT (Bands 2–3); and WorldView-2 (Bands 5–7). Blue line indicates the central wavelength of sensor bands while red line the optimum spectral regions for the detection of crop marks (700 nm and 800 nm).

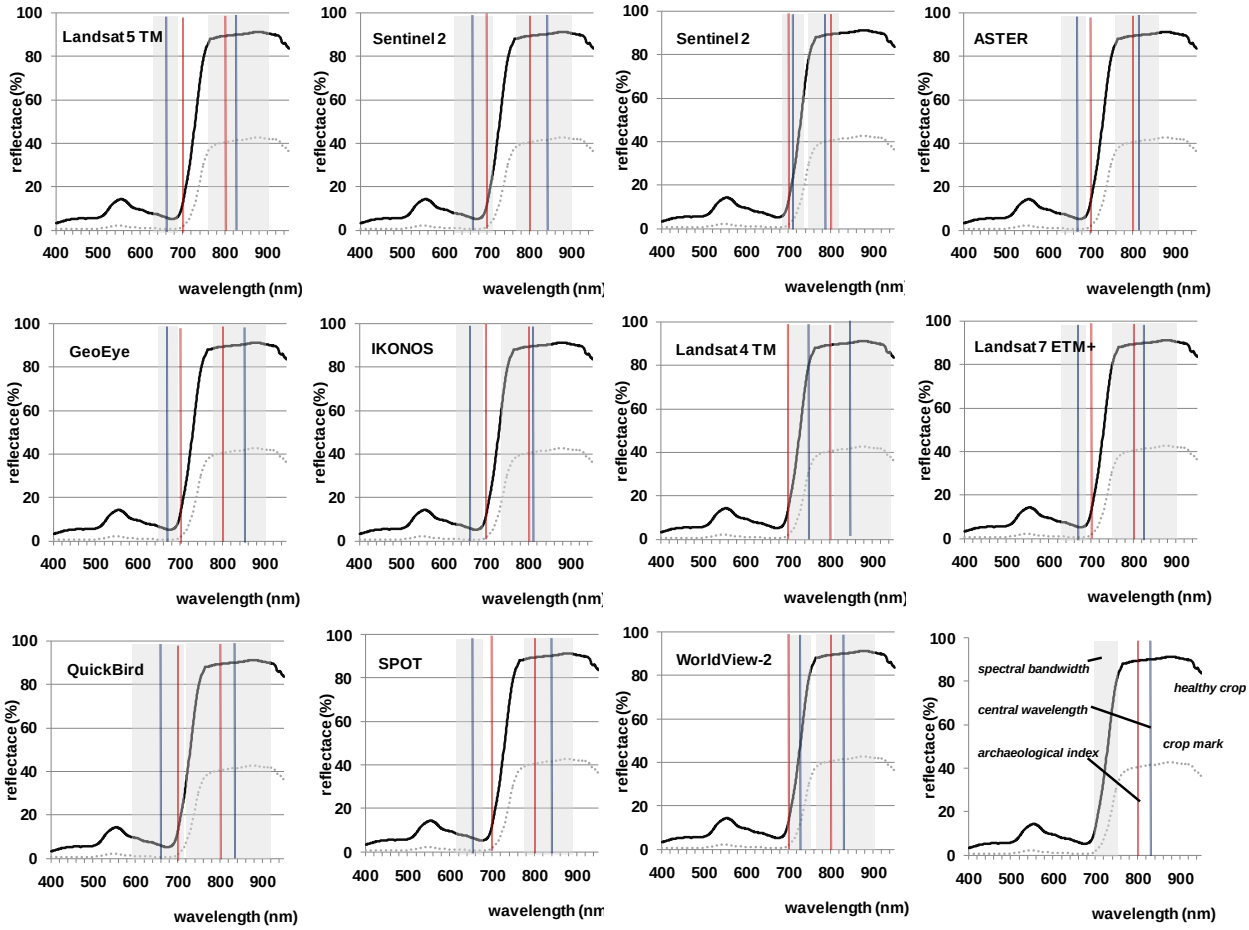

Figure 3. Relative Spectral Response of Sentinel-2 (Bands 1–8a). Typical spectral signatures of healthy crops and crop marks (dash line) are also shown.

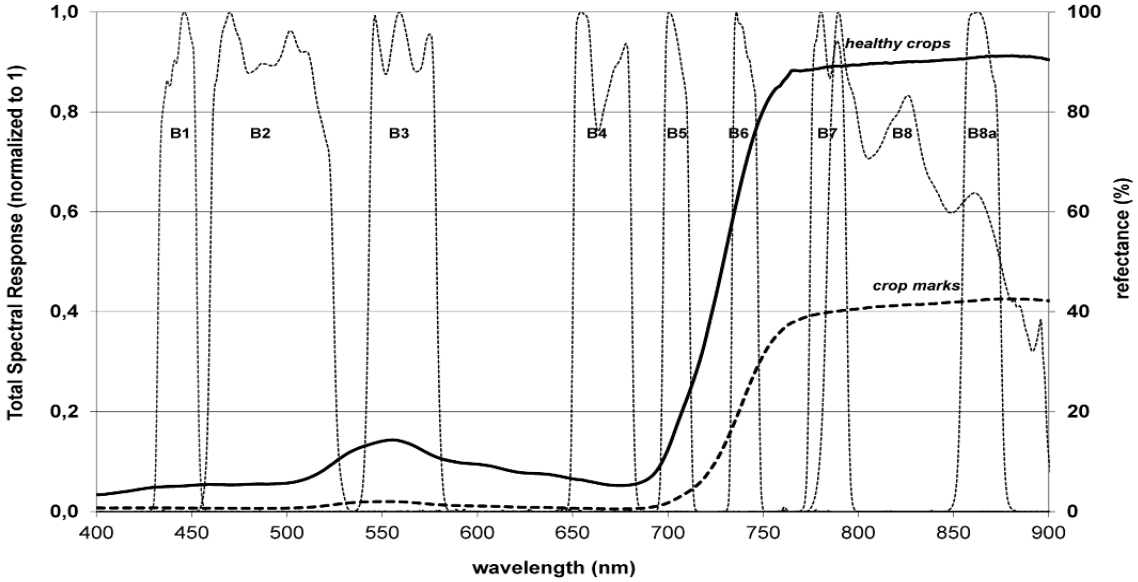

4.2. Relationship of Sentinel-2 Data with Archaeological Index

Based on the previous analysis, Sentinel-2 seems to have better spectral characteristics for the exposure of buried relics. In this section, a more detail analysis of the relationship of the simulated Sentinel-2 data with the Normalized Archaeological Index is provided. The equation of the Normalized Archaeological Index is shown below:

$$\text{Normalized Archaeological Index} = (p_{800} - p_{700})/(p_{800} + p_{700}) \quad (2)$$

where: p_{800}: reflectance at 800 nm; p_{700}: reflectance at 700 nm.

NDVI values for all sensors have been calculated based on the broadband simulated data. Narrowband reflectance values from the field spectroradiometric campaigns have been thoroughly resampled to all medium—and high-resolution satellite sensors mentioned in this study. Using these broadband reflectance values (Red and NIR bands), the NDVI was calculated. For Sentinel-2, the NDVI twice; once using Bands 4 and 8—as indicated by the Sentinel-2 User Guide—and secondly using Bands 5 and 7, which have similar spectral characteristics with the optimum archaeological spectral region. In addition, based on the narrowband reflectance of 700 nm and 800 nm the Normalized Archaeological Index was also retrieved.

A direct comparison of the NDVI and the Normalized Archaeological Index values is shown in Figure 4. Although similar values for both indices, and for all sensors, are found during the early and late phenological stages of the crops (*i.e.*, low NDVI values; NDVI < 0.20), significant variances are noted when the crops are fully vegetated (*i.e.*, high NDVI values; NDVI > 0.20). For all sensors, including the Sentinel-2 (Bands 4 and 8), a noteworthy difference is observed between the NDVI and the Normalized Archaeological Index. In contrast for Sentinel-2 (Bands 5 and 7) a good relationship is found.

Figure 4. NDVI values as retrieved from the different sensors mentioned in the study compared with the Normalized Archaeological Index.

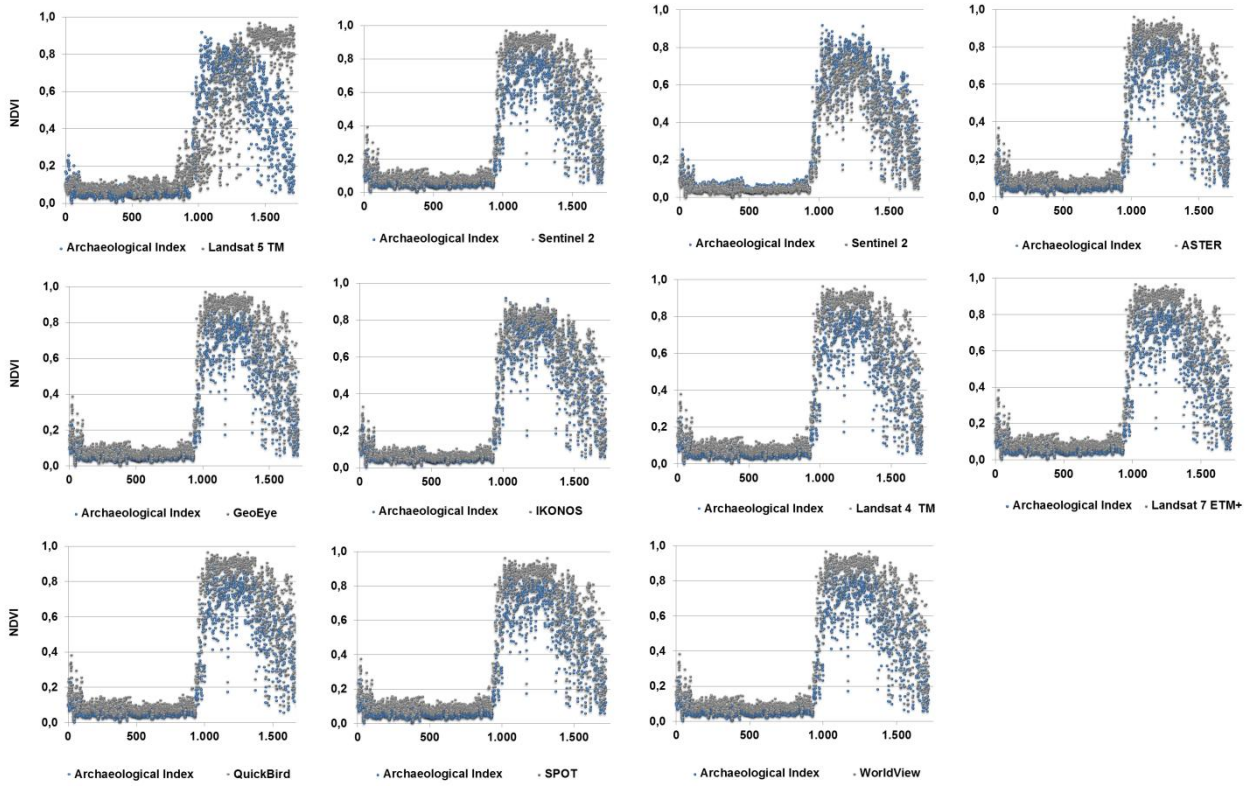

Relative differences between these two indices were calculated as it is shown in Figure 5. The differences for Sentinel-2 (Bands 5 and 7) were estimated at less than 10% for the whole phenological cycle. Contrary to this, ASTER, IKONOS, and QuickBird dataset, as well the Sentinel-2 (Bands 4 and 8) tend to give a relative difference of more than 20%. For the rest of the sensors (Landsat 4 TM+; Landsat 7 ETM+; SPOT; WorldView-2) this difference was calculated 30%, while for Landsat 5 TM this difference was more than 50%.

As is already known, the NDVI is estimated from the contribution of visible wavelength and near-infrared wavelengths. Strong and well-nourished vegetation absorbs most of the visible wavelengths that it receives, and reflects back a large proportion of the near-infrared radiation, whereas poor-condition vegetation, or thin areas, will reflect more visible wavelength light and less near-infrared light. For Sentinel-2, the NDVI ratio is based on the reflectance values of Band 8 (NIR) and Band 4 (Red). However, for an archaeological perspective, a strong relationship between the NDVI ratio using Bands 5 and 7 and the Archaeological Index is found. As it is presented in Figure 6, the NDVI index using the previous mentioned bands, tend to give a better statistical fit (r^2 = 0.96) against the Normalized Archaeological Index. Moreover, a small variance for the whole spectroradiometric dataset (*i.e.*, during the whole phenological cycle) is also noticed contrary to the published NDVI ratio of Sentinel-2.

Figure 5. Relative difference (%) of the NDVI values compared with the Normalized Archaeological Index.

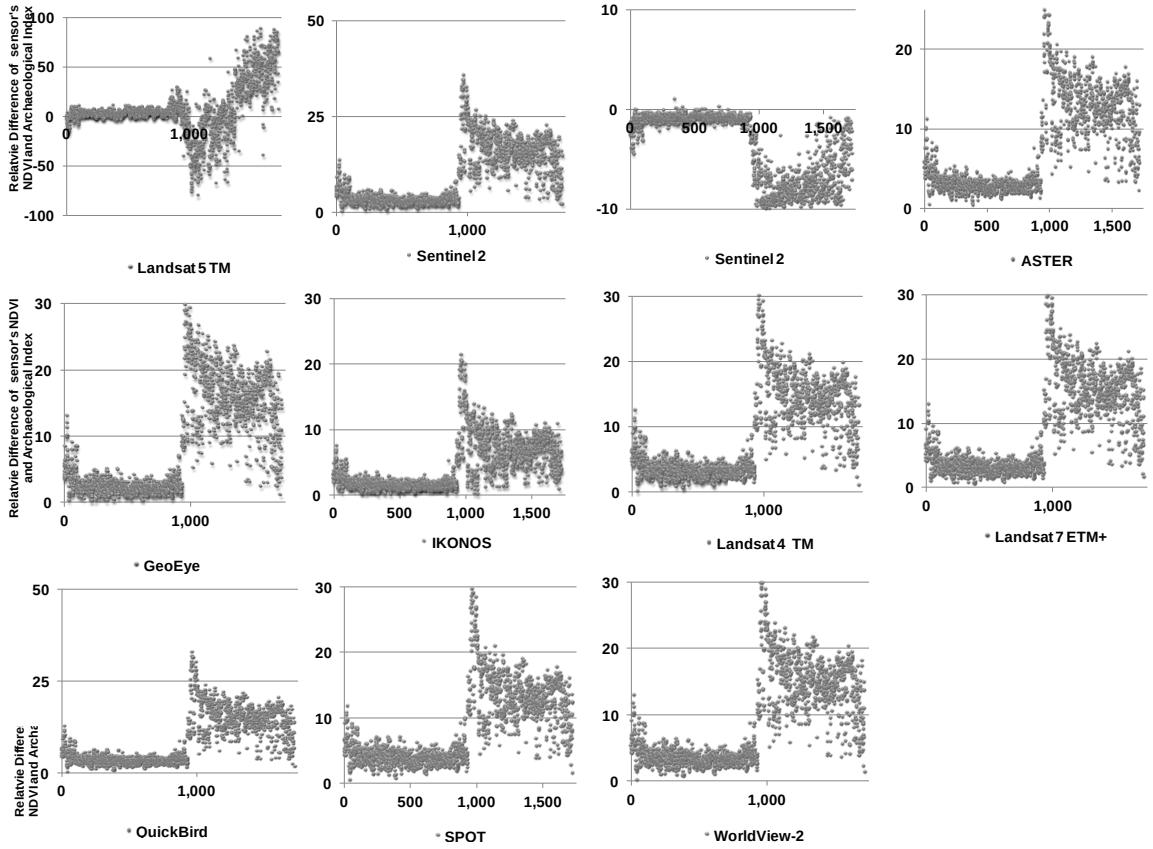

Figure 6. Best fit 2nd polynomial order of the Sentinel-2 NDVI compared to the Normalized Archaeological Index. NDVI was calculated using Bands 4 and 8, and Bands 5 and 7.

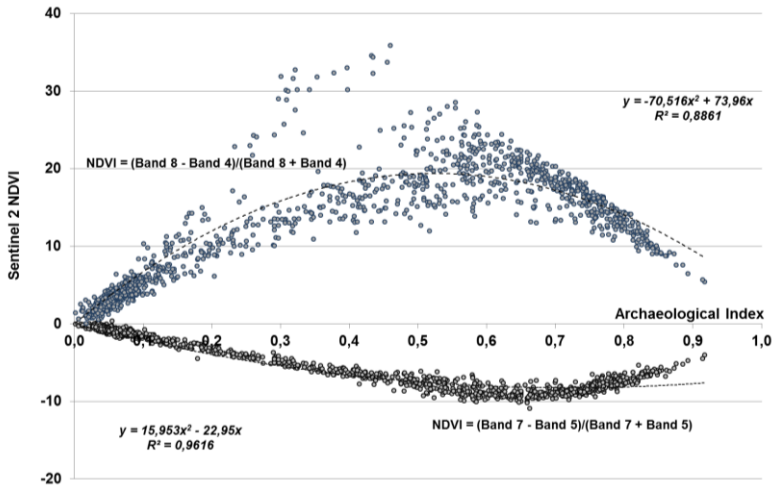

4.3. Performance of Sentinel-2 to Distinguish Vegetation Marks

The performance of Sentinel-2 sensor to distinguish vegetation marks was also examined using several existing broadband vegetation indices. As is known, vegetation indices intend to explore

vegetation's spectral signature characteristics, using visible and near infrared part of the spectrum. Canopy reflectance in the visible and near infrared is strongly dependent on both structural (*i.e*., amount of leaves per area, leaf orientation, canopy structure) and biochemical properties (*i.e*., chlorophylls, carotenoids) of the canopy [43]. Vegetation stress associated with sub-surface soil disturbance may be observed as visual symptoms, stunted growth, and sparse vegetation cover [44].

Even though several indices exist in the relevant literature only a small number of them has been practically used or evaluated for remote sensing archaeology applications. As was found [44], although NDVI is considered to be the most widely used index for archaeological studies, other existing vegetation indices might be also used successfully for the detection of buried archaeological relics.

Indeed more than hundred vegetation indices have been presented in the relevant literature, either using narrow-band or broad-band reflection [45]. In this section, some widely used vegetation indices applied for the enhancement of vegetation mark using satellite imagery have been evaluated (see Table 2 [46–58]). All these indices have been calculated for all sensors mentioned in this this study: Sentinel-2 (Bands 4–8); Sentinel-2 (Bands 5–7); Landsat 5 TM (Bands 3–4); ASTER (Bands 2–3); IKONOS (Bands 3–4); Landsat 4 TM (Bands 3–4); Landsat 7 ETM+ (Bands 3–4); QuickBird (Bands 3–4); SPOT (Bands 2–3); and WorldView-2 (Bands 5–7). The aim of this evaluation was to assess the potential of the new spectral characteristics of Sentinel-2 to further expand the capabilities of remote sensing techniques for the detection of buried archaeological features.

Table 2. Vegetation indices used in this study.

No	Vegetation Index	Equation	Reference
1	NDVI (Normalized Difference Vegetation Index)	$(p_{NIR} - p_{red})/(p_{NIR} + p_{red})$	[46]
2	Green NDVI (Green Normalized Difference Vegetation Index)	$(p_{NIR} - p_{green})/(p_{NIR} + p_{green})$	[47]
3	SR (Simple Ration)	p_{NIR}/p_{red}	[48]
4	MSR (Modified Simple Ratio)	$p_{red}/(p_{NIR} / p_{red} +1)^{0.5}$	[49]
5	MTVI2 (Modified Triangular Vegetation Index)	$[1.5(1.2 * (p_{NIR} - p_{green}) - 2.5(p_{Red} - p_{green})]/$ $[(2 p_{NIR} + 1)^2 - (6 p_{NIR} - 5 p_{Red}^{0.5}) - 0.5]^{0.5}$	[50]
6	RDVI (Renormalized Difference Vegetation Index)	$(p_{NIR} - p_{red})/(p_{NIR} + p_{red})^{1/2}$	[51]
7	IRG (Red Green Ratio Index)	$p_{Red} - p_{green}$	[52]
8	PVI (Perpendicular Vegetation Index)	$(p_{NIR} - \alpha p_{red} - b)/(1 + \alpha^2)$ $p_{NIR,soil} = \alpha p_{red,soil} + b$	[53]
9	RVI (Ratio Vegetation Index)	p_{red} / p_{NIR}	[54]
10	TSAVI (Transformed Soil Adjusted Vegetation Index)	$[\alpha(p_{NIR} - \alpha p_{NIR} - b)]/$ $[(p_{red} + \alpha p_{NIR} - \alpha b + 0.08(1 + \alpha^2))];$ $p_{NIR,soil} = \alpha p_{red,soil} + b$	[55]
11	MSAVI (Modified Soil Adjusted Vegetation Index)	$[2 p_{NIR} + 1 - [(2 p_{NIR} + 1)^2 - 8(p_{NIR} - p_{red})]^{1/2}]/2$	[56]
12	OSAVI (Optimized Soil Adjusted Vegetation Index)	$(p_{NIR} - p_{red})/(p_{NIR} + p_{red} +0.16)$	[57]
13	DVI (Difference Vegetation Index)	$p_{NIR} - p_{red}$	[58]

Following, relative difference between "vegetation marks" and the surrounding healthy vegetation using different vegetation indices was calculated (Table 3). As it was found from the results Sentinel-2 distinguished better vegetation marks from the surrounding vegetated area compared to the other sensors. Spectral characteristics of the forthcoming sensor seem to improve photointerpretation using either simple or more advance vegetation indices. It is interesting to note that, for the majority of indices examined in this study (≈85%), Sentinel-2 was the most suitable sensor for the detection of buried archaeological features. Moreover, Bands 5 and 7 of Sentinel-2, which were closed to the optimum spectral region for the detection of crop marks, tend to give high relative differences between "vegetation marks" and the surrounding healthy vegetation.

Table 3. Relative difference between "vegetation marks" and the surrounding healthy vegetation using different vegetation indices. The maximum difference for each index is underlined.

Vegetation Index Sensor	**NDVI**	**Green NDVI**	**SR**	**MSR**	**MTVI2**	**RDVI**	**IRG**	**PVI**	**RVI**	**TSAVI**	**MSAVI**	**OSAVI**	**DVI**
Landsat 5 TM	6	8	37	25	3	18	9	30	6	7	2	6	29
Sentinel-2 (Bands 4 and 8)	31	21	56	53	32	35	29	46	49	38	25	31	40
Sentinel-2 (Bands 5 and7)	38	22	39	54	64	42	3	61	30	54	31	38	48
ASTER	32	22	54	48	34	36	20	48	46	40	25	32	41
GeoEye	32	20	56	54	36	36	28	47	49	39	25	32	41
IKONOS	33	22	44	40	38	36	14	49	41	42	26	33	41
Landsat 4 TM	31	23	55	50	30	35	21	47	47	38	24	31	40
Landsat 7 ETM+	31	22	56	51	31	35	24	46	48	38	24	31	40
QuickBird	31	22	56	51	32	35	24	47	47	38	24	31	40
SPOT	30	20	54	47	33	34	20	46	45	38	24	30	40
WorldView-2	31	20	56	50	34	35	25	46	47	38	24	31	40

4.4. Simulation of Sentinel-2 for Archaeological Perspective

Previous studies from the authors [45,59,60] in the *Thessalian* region have shown that despite the low-resolution of the EO-Hyperion image, both broadband as well narrowband vegetation indices can be used for the detection of vegetation marks in this area. This mainly due to the size of the *tells* detected (>100 m radius). Therefore, in this paper, only the Archaeological Index is evaluated using the Sentinel-2 spectral characteristics.

As it was shown in the previous section, the Sentinel-2 dataset will be able to provide additional information for the detection of archaeological crop marks. Spectral characteristics of the specific sensor (Bands 5 and 7) are very similar with the spectral regions suitable for the detection of crop marks (700 nm and 800 nm). In this section, an attempt to simulate Sentinel-2 forthcoming products is presented.

For this aim, one EO-Hyperion image over the *Thessalian* plain (Central Greece) has been used. The EO-Hyperion narrow bands were resampled into the specific bandwidths of Bands 5 and 7 of the Sentinel-2 sensor using the relevant RSR filters. Specifically, the Hyperion Bands 33–36 and Bands 39–45 were resampled to Sentinel-2 Band 5 and 7, respectively.

In addition the spatial resolution of the EO-Hyperion was resampled to 20 m as in Sentinel-2. For this purpose, a high-resolution IKONOS image of the same area was acquired. A high relative geometric correction between the EO-Hyperion and the IKONOS image was achieved (Total Root Mean Square Error (TRMSE) < 2 m) using 2nd order polynomial order correction algorithm. Then, the IKONOS image was merged into the EO-Hyperion dataset using the PCA approach. This procedure was used in order to merge the high-resolution image (IKONOS, 1 m pixel size) with the lower-resolution image (EO-Hyperion, 30 m). Finally, the end product was resampled to 20 m as the Sentinel-2 spatial resolution.

As shown in Figure 7, some already known magoules (indicated with yellow color in Figure 7a,b were detected using simple photointerpretation of the image. These archaeological vegetation marks can be detected mainly due to the difference of the vegetation mark against the surrounding area, but also based on their circular shape. However, the most promising of this analysis was the detection of still unknown archaeological crops marks. Indeed, as demonstrated in Figure 7, at least another one potential site has been found in this area. The site (indicated with red color in Figure 7c) is in very close proximity to existing known sites and, therefore, the hypothesis of the existence of new sites is strengthened.

Figure 7. The simulated Sentinel-2 image over the *Thessalian* plain, based on the EO-Hyperion dataset. Known archaeological vegetation marks are indicated with yellow color, while another unknown vegetation mark is indicated in a red square.

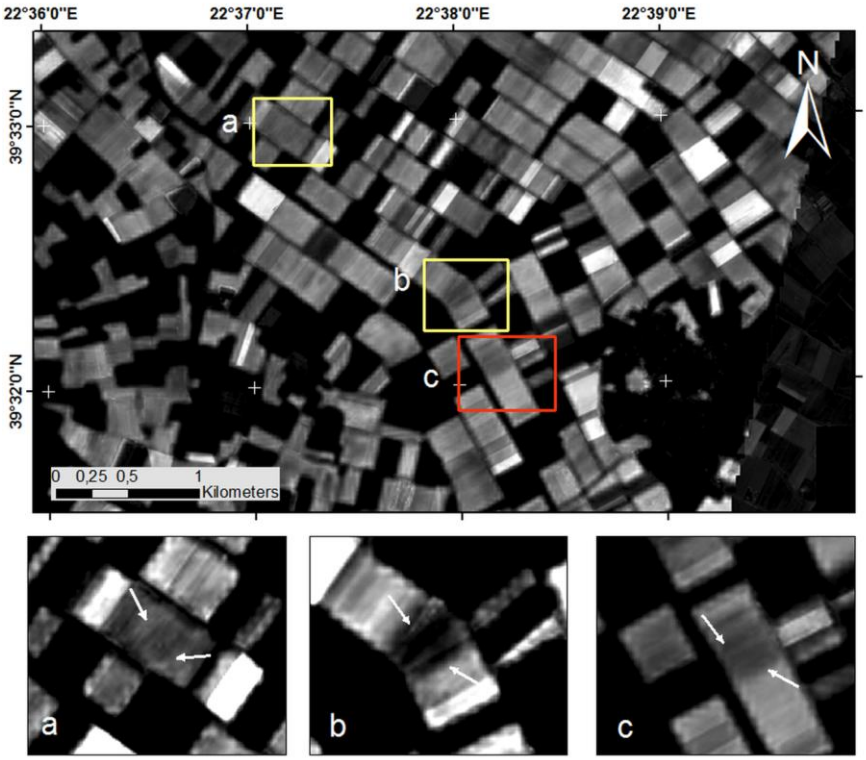

5. Conclusions

Satellite remote sensing provides new potential to the archaeological community. The discovery of new archaeological sites using such techniques has been already applied in several parts of the world. The discovery of new sites is mainly based on the detection of vegetation marks, which are formed due to the presence of buried archaeological relics. However, the detection of such crop marks is not considered to be an easy task.

In this study, the spectral capabilities of Sentinel-2 for archaeological perspective were examined. For this purpose, an extensive spectral library collected during a complete phenological cycle was evaluated. Further to the above-mentioned sensor, other existing and widely used satellite sensors have been also compared (Landsat 5 TM; ASTER; IKONOS; Landsat 4 TM; Landsat 7 ETM+; QuickBird; SPOT; and WorldView-2). All narrowband reflectance values taken from the *in situ* field campaigns have been resampled to all sensors using the appropriate RSR filters.

Formerly, Sentinel-2 was compared with the Archaeological Index, as well as with other vegetation indices. The results proved that specific bands of the new coming sensor (Bands 5 and 7) are very promising from an archaeological perspective. Indeed, these bands seem to have a good correlation with the Archaeological Index, but also can distinguish better crop marks from the surrounding vegetated area. In addition, a simulation of the sensor was made using one EO-Hyperion image over the *Thesssalian* plain. As it was found, the simulated Sentinel-2 sensor was able to detect not only known archaeological vegetation marks, but also some otherwise still unknown Neolithic tells.

From the outcomes of this study, it was found that Sentinel-2 is able to assist further the archaeological community. The new spectral capabilities of the forthcoming Sentinel-2, has attracted our interest, as some bandwidths of this sensor (Band 5 and 7) are closed to the optimum spectral regions for monitoring crop marks (700 nm and 800 nm). The Sentinel-2 is a European wide-swath, high-resolution, multi-spectral imaging mission, which is expected to be launched in 2014. The full mission specification of the twin satellites flying in the same orbit but phased at 180 °, is designed to give a high revisit frequency of five days at the Equator. It is also important to highlight that the Sentinel-2 mission will provide with important satellite products, freely available to scientific community, as well it continues existing the heritage missions of Landsat and SPOT space programs.

This is one of the first times that a satellite sensor is examined for its archaeological significance before its launch. Similar studies [61] can prepare the archaeological community for the advantages of forthcoming sensors, as well as to improve initiative for the generation of new algorithms for supporting archaeological perspective. Indeed, as is shown in this study, the simulated Sentinel-2 products are found to be very encouraging for archaeological investigations. The main disadvantage of the Sentinel-2 products is the low resolution (10–20 m), which in many cases can be problematic for the detection of buried archaeological remains. However, the Sentinel-2 dataset will be able to provide a better inside of the phenological changes of crops related with these remains and therefore to help researchers to understand better the formation of crop marks. This can be achieved based on, both, the temporal, as well the spectral, characteristics of the new sensor as the lately has been demonstrated in this study.

Acknowledgments

The authors would like to thank "Cyprus University of Technology Open Access Author Fund" for funding this publication. Special thanks are given to European Space Agency (ESA) for the provision of RSR filters of Sentinel-2. Moreover thanks are given to the 'Remote Sensing and Geo-Environment Lab' of the Department of Civil Engineering and Geomatics at the Cyprus University of Technology for the support

Author Contributions

Athos Agapiou conceived the study, collected field data, carried out the data analyses and wrote the manuscript. Dimitrios D. Alexakis, Apostolos Sarris and Diofantos G. Hadjimitsis validated the analysis and contributed significantly by suggestions and guidelines. All authors compiled and approved the final manuscript.

Conflicts of Interest

The authors declare no conflict of interest.

References

1. Jonson, K.J. *Remote Sensing in Archaeology: An Explicitly North America Perspective*; The University of Alabama Press: Tuscaloosa, AL, USA, 2006; p. 344.
2. Rowlands, A.; Sarris, A. Detection of exposed and subsurface archaeological remains using multi-sensor remote sensing. *J. Archaeol. Sci.* **2007**, *34*, 795–803.
3. Alexakis, D.; Sarris, A.; Astaras, T.; Albanakis, K. Detection of Neolithic settlements in Thessaly (Greece) through multispectral and hyperspectral satellite imagery. *Sensors* **2009**, *9*, 1167–1187.
4. Cavalli, R.M.; Colosi, F.; Palombo, A.; Pignatti, S.; Poscolieri, M. Remote hyperspectral imagery as a support to archaeological prospection. *J. Cult. Herit.* **2007**, *8*, 272–283.
5. Hadjimitsis, D.G.; Agapiou, A.; Alexakis, D.; Sarris, A. Exploring natural and anthropogenic hazard risk for cultural heritage in Cyprus using remote sensing and GIS. *Int. J. Digit. Earth* **2013**, *6*, 115–142.
6. De Laet, V.; Paulissen, E.; Waelkens, M. Methods for the extraction of archaeological features from very high-resolution Ikonos-2 remote sensing imagery, Hisar (southwest Turkey). *J. Archaeol. Sci.* **2007**, *34*, 830–841.
7. Banerjee, R.; Srivastava, K.P. Reconstruction of contested landscape: Detecting land cover transformation hosting cultural heritage sites from Central India using remote sensing. *Land Use Policy* **2013**, *34*, 193–203.
8. Lasaponara, R.; Masini, N. Satellite remote sensing in archaeology: Past, present and future perspectives. *J. Archaeol. Sci.* **2011**, *38*, 1771–1994.
9. Aqdus, A.S.; Hanson, S.W.; Drummond, J. The potential of hyperspectral and multi-spectral imagery to enhance archaeological cropmark detection: A comparative study. *J. Archaeol. Sci.* **2012**, *39*, 1915–1924.

10. Pappu, S.; Akhilesh, K.; Ravindranath, S.; Raj, U. Applications of satellite remote sensing for research and heritage management in Indian prehistory. *J. Archaeol. Sci*. **2010**, *37*, 2316–2331.
11. Agapiou, A.; Hadjimitsis, D.G. Vegetation indices and field spectro-radiometric measurements for validation of buried architectural remains: Verification under area surveyed with geophysical campaigns. *J. Appl. Remote Sens.* **2011**, *5*, doi:10.1117/1.3645590.
12. Parcak, S.H. *Satellite Remote Sensing for Archaeology*; Routledge Taylor and Francis Group Press: London, UK, 2009; p. 320.
13. Lasaponara, R.; Rosa, N. *Satellite Remote Sensing: A New Tool for Archaeology*; Springer: New York, NY, USA, 2012; p. 364.
14. Comer, D.; Harrower, M. *Mapping Archaeological Landscapes from Space*; Springer: New York, NY, USA, 2013; p. 276.
15. Lasaponara, R.; Masini, N. Detection of archaeological crop marks by using satellite QuickBird multispectral imagery. *J. Archaeol. Sci.* **2007**, *34*, 214–221
16. Altaweel, M. The use of ASTER satellite imagery in archaeological contexts. *Archaeol. Prospect.* **2005**, *12*, 151–166.
17. Sarris, A.; Papadopoulos, N.; Agapiou, A.; Salvi, M.C.; Hadjimitsis, D.G.; Parkinson, A.; Yerkes, R.W.; Gyucha, A.; Duffy, R.P. Integration of geophysical surveys, ground hyperspectral measurements, aerial and satellite imagery for archaeological prospection of prehistoric sites: The case study of Veszto-Magor Tell, Hungary. *J. Archaeol. Sci.* **2013**, *40*, 1454–1470.
18. Noviello, M.; Ciminale, M.; de Pasquale, V. Combined application of pansharpening and enhancement methods to improve archaeological cropmark visibility and identification in QuickBird imagery: Two case studies from Apulia, Southern Italy. *J. Archaeol. Sci.* **2013**, *40*, 3604–3613.
19. Gojda, M.; Hejcman, M. Cropmarks in main field crops enable the identification of a wide spectrum of buried features on archaeological sites in Central Europe. *J. Archaeol. Sci.* **2012**, *39*, 1655–1664.
20. Agapiou, A.; Hadjimitsis, D.G.; Sarris, A.; Georgopoulos, A.; Alexakis, D.D. Optimum temporal and spectral window for monitoring crop Marks over archaeological remains in the Mediterranean region. *J. Archaeol. Sci.* **2013**, *40*, 1479–1492.
21. Agapiou, A.; Alexakis, D.D.; Hadjimitsis, D.G. Spectral sensitivity of ALOS, ASTER, IKONOS, LANDSAT and SPOT satellite imagery intended for the detection of archaeological crop marks. *Int. J. Digit. Earth* **2012**, doi:10.1080/17538947.2012.674159.
22. Winton, H.; Horne, P. C. National Archives for National Survey Programmes: NMP and the English Heritage Aerial Photograph Collection. In *Landscapes through the Lens*; Aerial Archaeology Research Group: Emporia, KS, USA, 2010; Volume 2, pp. 7–18.
23. Riley, D.N. Factors in the development of crop marks. *Aerial Archaeol.* **1979**, *4*, 28–32.
24. Sharpe, L. *Geophysical, Geochemical and Arable Crop Responses to Archaeological Sites in the Upper Clyde Valley, Scotland*; University of Glasgow: Glasgow, UK, 2004.
25. Hejcman, M.; Smrz, Z. Crop marks in stands of cereals, legumes and winter rape indicate sub-soil archaeological features in the agricultural landscape of Central Europe. *Agric. Ecosyst. Environ.* **2010**, *138*, 348–354.

26. Agapiou, A.; Hadjimitsis, D.G.; Alexakis, D.D. Development of an image-based method for the detection of archaeological buried relics using multi-temporal satellite imagery. *Int. J. Remote Sens.* **2013**, *34*, 5979–5996.
27. Agapiou, A.; Hadjimitsis, D.G.; Alexakis, D.D.; Papadavid, G. Examining the phenological cycle of barley (hordeum vulgare) using satellite and *in situ* spectroradiometer measurements for the detection of buried archaeological remains. *GISci. Remote Sens.* **2012**, *49*, 854–872.
28. Cavalli, R.M.; Licciardi, G.A; Chanussot, J. Detection of anomalies produced by buried archaeological structures using nonlinear principal component analysis applied to airborne hyperspectral image. *IEEE J. Sel. Top. Appl. Earth Observ. Remote Sens.* **2013**, *6*, 659–669.
29. Bassani, C.; Cavalli, R.M.; Goffredo, R.; Palombo, A.; Pascucci, S.; Pignatti, S. Specific spectral bands for different land cover contexts to improve the efficiency of remote sensing archaeological prospection: The Arpi case study. *J. Cult. Herit.* **2009**, *10*, e41–e48.
30. Cavalli, R.M.; Pascucci, S.; Pignatti, S. Optimal spectral domain selection for maximizing archaeological signatures: Italy case studies. *Sensors* **2009**, *9*, 1754–1767.
31. Agapiou, A.; Hadjimitsis. D.G.; Georgopoulos, A.; Sarris, A.; Alexakis, D.D. Towards to an archaeological index: Identify the spectral regions of stress vegetation due to buried archaeological remain. *Lect. Notes Comput. Sci.* **2012**, *7616*, 129–138.
32. Drusch, M.; del Bello, U.; Carlier, S.; Colin, O.; Fernandez, V.; Gascon, F.; Hoersch, B.; Isola, C.; Laberinti, P.; Martimort, P.; *et al.* Sentinel-2: ESA's optical high-resolution mission for GMES operational services. *Remote Sens. Environ.* **2012**, *120*, 25–36.
33. Malenovsky, Z.; Rott, H.; Cihlar, J.; Schaepman, E.M.; Garcia-Santos, G.; Fernandes, R.; Berger, M. Sentinels for science: Potential of Sentinel-1, -2, and -3 missions for scientific observations of ocean, cryosphere, and land. *Remote Sens. Environ.* **2012**, *120*, 91–101.
34. Berger, M.; Moreno, J.; Johannessen, A.J.; Levelt, F.P.; Hanssen, F.R. ESA's sentinel missions in support of earth system science. *Remote Sens. Environ.* **2012**, *120*, 84–90.
35. Fletcher, K. *Sentinel-2: ESA's Optical High-Resolution Mission for GMES Operational Services*; ESA Communications: Noordwijk, The Netherlands, 2012.
36. Honkavaara, E.; Markelin, L.; Rosnell, T.; Nurminen, K. Influence of solar elevation in radiometric and geometric performanceof multispectral photogrammetry. *ISPRS J. Photogramm. Remote Sens.* **2012**, *67*, 13–26.
37. Milton, E.J.; Schaepman, M.E.; Anderson, K.; Kneubuhler, M.; Fox, N. Progress in field spectroscopy. *Remote Sens. Environ.* **2009**, *113*, 92–109.
38. Alexakis, A.; Sarris, A.; Astaras, T.; Albanakis, K. Integrated GIS, remote sensing and geomorphologic approaches for the reconstruction of the landscape habitation of Thessaly during the neolithic period. *J. Archaeol. Sci.* **2011**, *38*, 89–100.
39. Frampton, J.W.; Dash, J.; Watmough, G.; Milton, J.E. Evaluating the capabilities of Sentinel-2 for quantitative estimation of biophysical variables in vegetation. *ISPRS J. Photogramm. Remote Sens.* **2013**, *82*, 83–92.
40. Herrmann, I.; Pimstein, A.; Karnieli, A.; Cohen, Y.; Alchanatis, V.; Bonfil, D.J. LAI assessment of wheat and potato crops by VENμS and Sentinel-2 bands. *Remote Sens. Environ.* **2011**, *115*, 2141–2151.

41. Trishchenko, P.A.; Cihlar, J.; Li, Z. Effects of spectral response function on surface reflectance and NDVI measured with moderate resolution satellite sensors. *Remote Sens. Environ.* **2002**, *81*, 1–18.
42. Verhoeven, G.; Doneus, M. Balancing on the borderline—A low cost approach to visualize the red- edge shift for the benefit of the aerial archaeology. *Archaeol. Prospect.* **2011**, *18*, 267–278.
43. Stagakis, S.; Markos, N.; Sykioti, O.; Kyparissis, A. Monitoring canopy biophysical and biochemical parameters in ecosystem scale using satellite hyperspectral imagery: An application on a *Phlomis fruticosa* Mediterranean ecosystem using multiangular CHRIS/PROBA observations. *Remote Sens. Environ.* **2010**, *114*, 977–994.
44. White, D.C.; Williams, M.; Barr, S.L. Detecting sub-surface soil disturbance using hyperspectral first derivative band rations of associated vegetation stress. *Int. Arch. Photogramm. Remote Sens. Spat. Inf. Sci.* **2008**, *XXXVII*, 243–248.
45. Agapiou, A.; Hadjimitsis, D.G.; Alexakis, D.D. Evaluation of broadband and narrowband vegetation indices for the identification of archaeological crop marks. *Remote Sens.* **2012**, *4*, 3892–3919.
46. Rouse, J.W.; Haas, R.H.; Schell, J.A.; Deering, D.W.; Harlan, J.C. *Monitoring the Vernal Advancements and Retrogradation. (Greenwave. Effect) of Nature Vegetation*; NASA/GSFC Final Report; NASA: Greenbelt, MD, USA, 1974.
47. Gitelson, A.A.; Kaufman, Y.J.; Merzlyak, M.N. Use of a green channel in remote sensing of global vegetation from EOS-MODIS. *Remote Sens. Environ.* **1996**, *58*, 289–298.
48. Jordan, C.F. Derivation of leaf area index from quality of light on the forest floor. *Ecology* **1969**, *50*, 663–666.
49. Chen, J.M. Evaluation of vegetation indices and a modified simple ratio for Boreal application, *Can. J. Remote Sens.* **1996**, *22*, 229–242.
50. Haboudane, D.; Miller, J.R.; Pattey, E.; Zarco-Tejada; P.; Strachan, I.B. Hyperspectral vegetation indices and novel algorithms for predicting green LAI of crop canopies: Modeling and validation in the context of precision agriculture. *Remote Sens. Environ.* **2004**, *90*, 337–352.
51. Roujean, J.L.; Breon, F.M. Estimating PAR absorbed by vegetation from bidirectional reflectance measurements. *Remote Sens. Environ.* **1995**, *51*, 375–384.
52. Gamon, J.A.; Surfus, J.S. Assessing leaf pigment content and activity with a reflectometer. *New Phytologist.* **1999**, *143*, 105–117.
53. Richardson, A.J.; Wiegand, C.L. Distinguishing vegetation from soil background information. *Photogram. Eng. Remote Sensing.* **1977**, *43*, 15–41.
54. Pearson, R.L.; Miller, L.D. Remote Mapping of Standing Crop Biomass and Estimation of the Productivity of the Short Grass Prairie, Pawnee National Grasslands, Colorado. In Proceedings of the 8th International Symposium on Remote Sensing of the Environment, Ann Arbor, MI, USA, 2–6 October 1972.
55. Baret, F.; Guyot, G. Potentials and limits of vegetation indices for LAI and APAR assessment. *Remote Sens. Environ.* **1991**, *35*, 161–173.
56. Qi, J.; Chehbouni, A.; Huete, A.R.; Kerr, Y.H.; Sorooshian, S. A modified soil adjusted vegetation index. *Remote Sens. Environ.* **1994**, *48*, 119–126.

57. Rondeaux, G.; Steven, M.; Baret, F. Optimization of soil-adjusted vegetation indices. *Remote Sens. Environ.* **1996**, *55*, 95–107.
58. Tucker, C.J. Red and photographic infrared linear combinations for monitoring vegetation. *Remote Sens. Environ.* **1979**, *8*, 127–150.
59. Agapiou, A.; Alexakis, D.D.; Stavrou, M.; Sarris, A.; Themistocleous, K.; Hadjimitsis, D.G. Prospects and Limitations of Vegetation Indices in Archaeological Research: The Neolithic Thessaly Case Study. In Proceedings of SPIE 8893, Earth Resources and Environmental Remote Sensing/GIS Applications IV, Dresden, Germany, 24 October 2013.
60. Linear Spectral Unmixing for the detection of Neolithic Settlements in the Thessalian Plain, Central Greece. Available online: http://www.earsel.org/symposia/2012-symposium-Mykonos/Proceedings/04-05_EARSeL-Symposium-2012.pdf (accessed on 15 January 2014).
61. Cavalli, R.M.; Betti, M.; Campanelli, A.; Cicco, A.D.; Guglietta, D.; Penna, P.; Piermattei, V. A methodology to assess the accuracy with which remote data characterize a specific surface, as a Function of Full Width at Half Maximum (FWHM): Application to three Italian coastal waters. *Sensors* **2014**, *14*, 1155–1183.